Hindawi
Journal of Control Science and Engineering
Volume 2017, Article ID 3169172, 8 pages
https://doi.org/10.1155/2017/3169172

Research Article

Tooth Fracture Detection in Spiral Bevel Gears System by Harmonic Response Based on Finite Element Method

Yuan Chen,[1,2] Rupeng Zhu,[1] Guanghu Jin,[1] and Yeping Xiong[2]

[1] *College of Mechanical and Electrical Engineering, Nanjing University of Aeronautics and Astronautics, Nanjing 210016, China*
[2] *Engineering and Environment, University of Southampton, Boldrewood Innovation Campus, Southampton SO16 7QF, UK*

Correspondence should be addressed to Rupeng Zhu; rpzhu@nuaa.edu.cn

Received 11 August 2017; Revised 11 October 2017; Accepted 19 October 2017; Published 3 December 2017

Academic Editor: Zhixing Cao

Spiral bevel gears occupy several advantages such as high contact ratio, strong carrying capacity, and smooth operation, which become one of the most widely used components in high-speed stage of the aeronautical transmission system. Its dynamic characteristics are addressed by many scholars. However, spiral bevel gears, especially tooth fracture occurrence and monitoring, are not to be investigated, according to the limited published issues. Therefore, this paper establishes a three-dimensional model and finite element model of the Gleason spiral bevel gear pair. The model considers the effect of tooth root fracture on the system due to fatigue. Finite element method is used to compute the mesh generation, set the boundary condition, and carry out the dynamic load. The harmonic response spectra of the base under tooth fracture are calculated and the influence of main parameters on monitoring failure is investigated as well. The results show that the change of torque affects insignificantly the determination of whether or not the system has tooth fracture. The intermediate frequency interval (200 Hz–1000 Hz) is the best interval to judge tooth fracture occurrence. The best fault test region is located in the working area where the system is going through meshing. The simulation calculation provides a theoretical reference for spiral bevel gear system test and fault diagnosis.

1. Introduction

Spiral bevel gears are one of the most important components of the aeronautical transmission system. Due to the harsh working environment, failure occurs sometimes, and the most common situation is resonance failure. The failure of the spiral bevel gear transmission system often leads to serious accidents; therefore, accurate detection, the positioning of the fault, and eliminating hidden danger have very important significance in improving the operating efficiency of the gear system.

Most studies were related to spiral bevel gear modeling and tooth contact analysis (TCA); Tsai and Chin [1] developed mathematical modeling of the tooth surface geometry for bevel gear pairs based on the basic gearing kinematics and involute geometry along with the tangent planes geometry. Litvin et al. [2–6] proposed an integrated computerized approach for spiral bevel gear drives and simulated mesh and contact stress analysis; they reduced the magnitude of transmission errors for reduction of noise and vibration and found severe contact stresses areas to increase the endurance of the gear drives; the proposed results were proved by the manufacturing and test of prototypes. Sheveleva et al. [7, 8] developed a modified computer program for tooth contact analysis (TCA) for the most general case and provided computer codes for contact path, bearing contact, and contact pressure distribution. Simon [9] presented computer aided tooth contact analysis in mismatched spiral bevel gears and discussed the influence of relative position errors of meshing pinion on tooth contact.

About spiral bevel gear fault detection, Zakrajsek et al. [10] applied a variety of gear fault detection techniques to investigate the growth and propagation of the fault; the relationship between the system running time and pinion damage was specified as well. Dempsey et al. [11] developed the diagnostic tool by collecting vibration and oil debris data from fatigue tests performed in Glenn spiral bevel gear fatigue rigs. Decker and Lewicki [12] discussed the

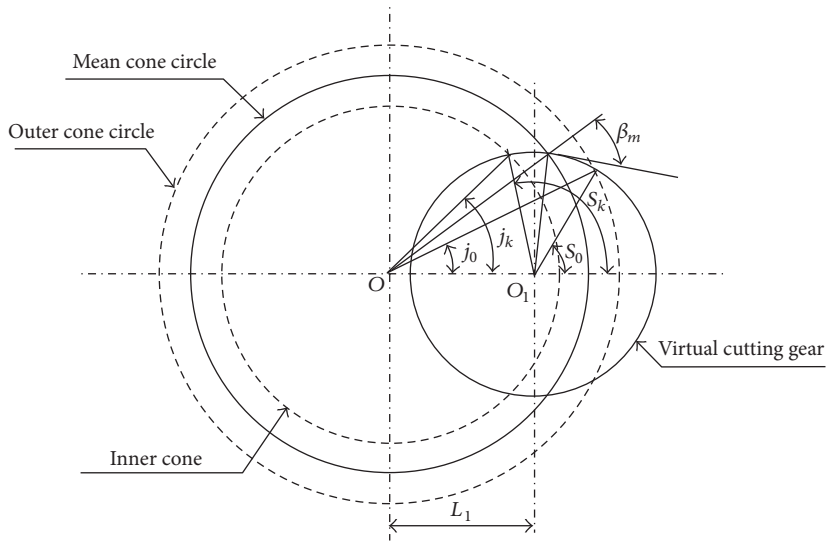

Figure 1: Pitch surface unfolded map.

damage detection effectiveness of the different metrics and a comparison of effects of different accelerometer locations by spiral bevel pinion running test. Ural et al. [13] predicted the crack shape and fatigue life for a spiral bevel pinion gear by using computational fracture mechanics, which was based on linear elastic fracture mechanics theories combined with finite element method. However, the detection in the frequency domain and the influence of excitation were not provided in these papers.

In the area of spiral gear dynamics analysis, Li and Hu [14] analyzed the axial–lateral–torsional coupled spiral bevel geared system theoretically and the dynamic behavior of the system was investigated by numerical method. Yinong et al. [15] studied the effect of the asymmetric mesh stiffness on the 8-DOF spiral bevel gear transmission system. Feng and Song [16] investigated the effects of the dynamic meshing force and dynamic transmission error.

Therefore, through system vibration signal to determine the occurrence of tooth fracture, thus eliminating the fault, is a meaningful work. In this paper, a pair of Gleason spiral bevel gears is mathematically modeled and a three-dimensional solid model is generated as well. Finite element method is applied to analyze the harmonic response of the system; deformation amplitude and phase of the base are calculated. Therefore some tooth fracture features and main parameters' influences are analyzed to assist the fault recognition.

2. System Modeling

2.1. Three-Dimensional Precise Solid Modeling. Typical spiral bevel gears applied in aeronautical transmission system are manufactured by Gleason face hobbing process [17]. The tooth profile of the spiral bevel gear is a spherical involute, and its tooth profile is circular, and the tooth surface is a complex three-dimensional surface. Therefore, the method of modeling the cylindrical gear tooth profile is not suitable for the spiral bevel gear. By adding the auxiliary involute to the tooth line equation, the accuracy of the tooth surface could be increased.

In the spherical coordinate system, the spherical involute equation on one side of outer space width is

$$\begin{aligned} r &= R \\ \theta &= \delta_f + t\left(\delta_a - \delta_f\right) \\ \varphi &= \frac{\arccos\left(\cos\theta/\cos\delta_b\right)}{\sin\delta_b} - \arccos\left(\frac{\tan\delta_b}{\tan\theta}\right), \end{aligned} \tag{1}$$

where δ_b is base angle; δ_f is root angle; δ_a is tip angle; R is sphere radius, that is, outer cone distance.

The spherical involute equation on the other side of outer space width is

$$\begin{aligned} r &= R \\ \theta &= \delta_f + t\left(\delta_a - \delta_f\right); \\ \varphi &= \frac{\arccos\left(\cos\theta/\cos\delta_b\right)}{\sin\delta_b} - \arccos\left(\frac{\tan\delta_b}{\tan\theta}\right) \\ &\quad - \left(\frac{360}{z} - \phi_b\right) \end{aligned} \tag{2}$$

here, z is tooth number; φ_b is tooth thickness base angle.

When spiral bevel gears are in cutting processing, tooth pitch surface unfolded drawing is shown in Figure 1.

The distance between cutting tool circle O_1 and cone circle O is depicted as

$$L_1 = \sqrt{{R_m}^2 + {R_d}^2 - 2R_m R_d \sin\beta_m}, \tag{3}$$

where β_m is mean spiral angle; R_m is mean cone distance; R_d is the radius of cutting tool.

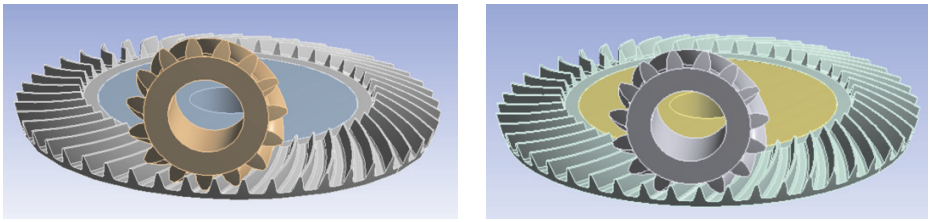

(a) Healthy model (b) Tooth fracture model

Figure 2: Spiral bevel gear assembly model.

In circle O_1, offset angle S_0 of outer cone circle and S_k of inner cone circle are

$$S_0 = 180 - \arccos\frac{L_1 + {R_d}^2 - R^2}{2L_1R_d}$$
$$S_k = 180 - \arccos\frac{L_1 + {R_d}^2 - (R-B)^2}{2L_1R_d}; \quad (4)$$

here, B is tooth thickness.

In circle O, offset angle j_0 of outer cone circle and j_k of inner cone circle are

$$j_0 = \arctan\frac{R_d \sin S_0}{L_1 + R_d \cos S_0}$$
$$j_k = \arctan\frac{R_d \sin S_k}{L_1 + R_d \cos S_k}. \quad (5)$$

According to the spherical geometrical relationship, spherical angle q corresponding to plane angle j could be

$$q_0 = \frac{j_0}{\sin\delta}$$
$$q_k = \frac{j_k}{\sin\delta}; \quad (6)$$

here, δ is reference cone angle.

Thus, $q_{0k} = q_k - q_0$, that is, the rotation angle between outer cone and inner cone in the spherical coordinate system.

The spherical involute equation on one side of inner space width could be derived by substituting r to (R-B) and adding the value of φ to q_{0k} in (1). Similarly, involute equation on the other side of inner space width could be deduced as well.

In order to improve the accuracy of the three-dimensional model, in this paper, a number of equally spaced auxiliary spherical involute lines are inserted in the direction of the tooth line. Substitute (R-B) to (R-0.1nB) in (1) and (4), and n is followed by $1, 2, 3 \ldots 9 \ldots$, then involute equation could be rederived.

Based on the above-mentioned involute equation, key points of the curve are established by "law command" in CATIA. Then "spline command" is applied to connect these key points for the tooth profile involute curve, and "multisection surface command" is used to generate the tooth surface. Moreover, tooth space is modeled by "split command," which is based on these tooth surfaces. Finally, with the Boolean subtraction calculation of the solids, the parametric modeling of the spiral bevel gear could be successfully achieved, which verifies the correctness of the design method [18].

Table 1: System parameters.

	Active gear	Driven gear
Modulus	6	
Pressure angle (°)	20	
Tooth number	15	46
Tooth width (m)	0.44	0.44
Shaft angle Σ(°)	90	
Mean spiral angle (°)	35	

In addition, due to long-term operation in the high-speed circumstance, tooth root is prone to fatigue fracture. This paper simulates the fractured tooth and completes the healthy and fracture spiral bevel gear assembly model, as shown in Figure 2; main parameters are listed in Table 1.

2.2. Finite Element Meshing and Pretreatment Process. The geometric model in CATIA is introduced into ANSYS workbench 18.1, so finite element analysis model is obtained. As friction contact analysis is a nonlinear problem, in order to save the computing resources and improve calculation accuracy, hexahedral meshing method is applied for calculation, and then the grid is refined in contact areas. The grid size of the noncontact region of this model is defined as 5 mm, and the contact area is defined as 1 mm, which ensures the rationality of the mesh and the maximum efficiency. At the same time, in order to ensure the convergence of the calculation results, the meshing model is firstly calculated, and then the mesh size of the contact area is gradually reduced. If the difference between calculation results is small after multiple attempts, the result is convergent and acceptable. Figure 3 shows the meshing model of spiral bevel gear pair; the results tend to converge when the number of nodes is 151443 and the number of elements is 47982 in healthy model; the number of nodes is 151749 and the number of elements is 47728 in tooth fracture model.

After mesh is complete, the model is processing multiple settings, that is, pretreatment process:

(1) Material definition: the model is set according to steel properties, the active and driven gears belong to

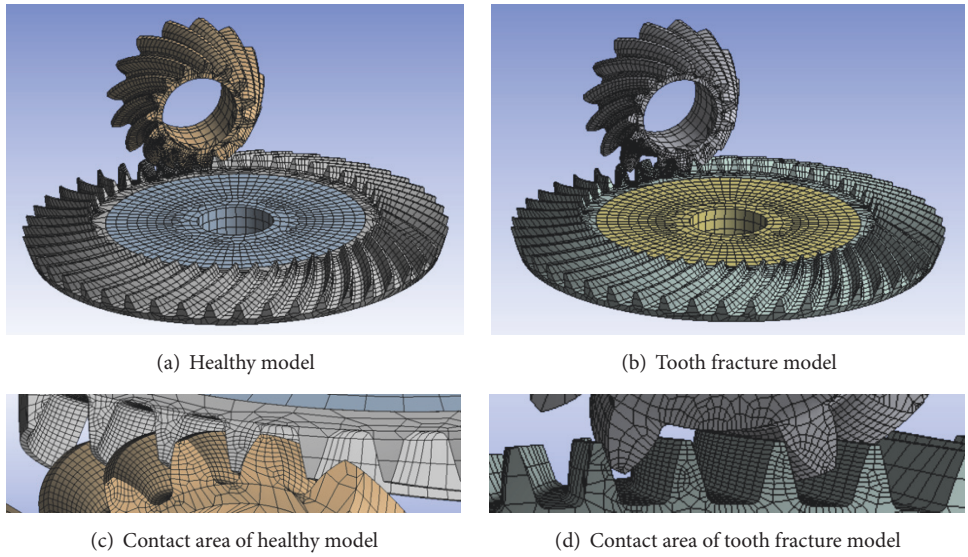

(a) Healthy model (b) Tooth fracture model

(c) Contact area of healthy model (d) Contact area of tooth fracture model

Figure 3: Spiral bevel gear meshing.

the same material, Young's modulus is 2.1×10^{11} Pa, Poisson's ratio is 0.3, and the density is 7850 kg/m^3.

(2) Contact definition: the calculation of the spiral bevel gear pair is surface-to-surface contact problem between the elastomers. It is of great importance to select contact surface and target surface; the inappropriate selection will lead to excessive penetration, affecting the accuracy of the solution. In general, when the convex and concave surfaces contact, the concave surface should be set as the target surface, so the spiral bevel gear outer tooth surface is defined as the target surface. In addition, the amount of penetration between the two contact surfaces depends on the normal contact stiffness. If the normal contact stiffness is too large, it will increase solution iteration number, which may lead to nonconvergence; if the normal contact stiffness is too small, the penetration between nodes could be too large, resulting in model instability. Based on the above analysis, this paper firstly uses the small normal contact stiffness coefficient and then gradually increases until analysis results deviation is so small. The results show that the best normal contact stiffness coefficient is 1.0 when the normal contact stiffness coefficient is set from 0.001, 0.01, 0.1, 1.0, and 1.1.

(3) Rotational pair definition: the inner surfaces of the gears are set as reference surfaces, and then the rotational centers of reference surfaces are created. Finally, a pair of rotational gears is defined.

(4) Solver definition: the general equation for harmonic response analysis is

$$[M]\left\{\ddot{X}\right\} + [C]\left\{\dot{X}\right\} + [K]\{X\} = \{F\}, \quad (7)$$

where $[M]$, $[C]$, and $[K]$ are the mass matrix, damping matrix, and stiffness matrix of the system. Matrix $[F]$ is external excitation and is equal to $F_0 \cos(\omega t)$.

The time-varying meshing stiffness, meshing line displacement, and dynamic meshing force can be regarded as periodic format and can be expanded in Fourier series under fundamental meshing frequency. In this paper, dynamic meshing force is simulated as the excitation load, the torque is loaded in the sinusoidal form, the sweep frequency is set from 0 to 2000 Hz, initial phase angle is 0°, and solution intervals are 100.

(5) Boundary conditions and load setting: degree of freedom (DOF) is released only in rotational direction, and the value of torque is 1200 N·m, which is gradually applied on the active gear.

3. Fault Diagnosis Analysis

3.1. Tooth Fracture Detection. The system is solved by the augmented Lagrangian method in ANSYS and the first six natural frequencies of the system are obtained, as shown in Table 2. As illustrated in the table, the natural frequency of the tooth fracture model decreases in each order; the frequency deviation of the fourth and sixth order is relatively large.

The base of the driven gear is the optimum position for deformation vibration detection sensor and acceleration vibration detection sensor so that the base is also set in response to the output in finite element method. Figure 4 shows the calculated deformation and acceleration harmonic response maps.

Here, in order to separate ideal monitoring frequency, three frequency intervals are defined to describe the sweep frequency, that is, low frequency interval (below than 200 Hz), intermediate frequency interval (200 Hz to 1000 Hz), and high frequency interval (greater than 1000 Hz) [19].

Table 2: Natural frequency.

Order	Healthy tooth model frequency (Hz)	Fracture tooth model frequency (Hz)	Deviation (Hz)
(1)	18.4	12.0	6.4
(2)	168.0	140.8	27.2
(3)	206.5	147.3	59.2
(4)	678.1	571.6	106.5
(5)	1061.2	1042.4	18.8
(6)	1543	1367.3	175.7

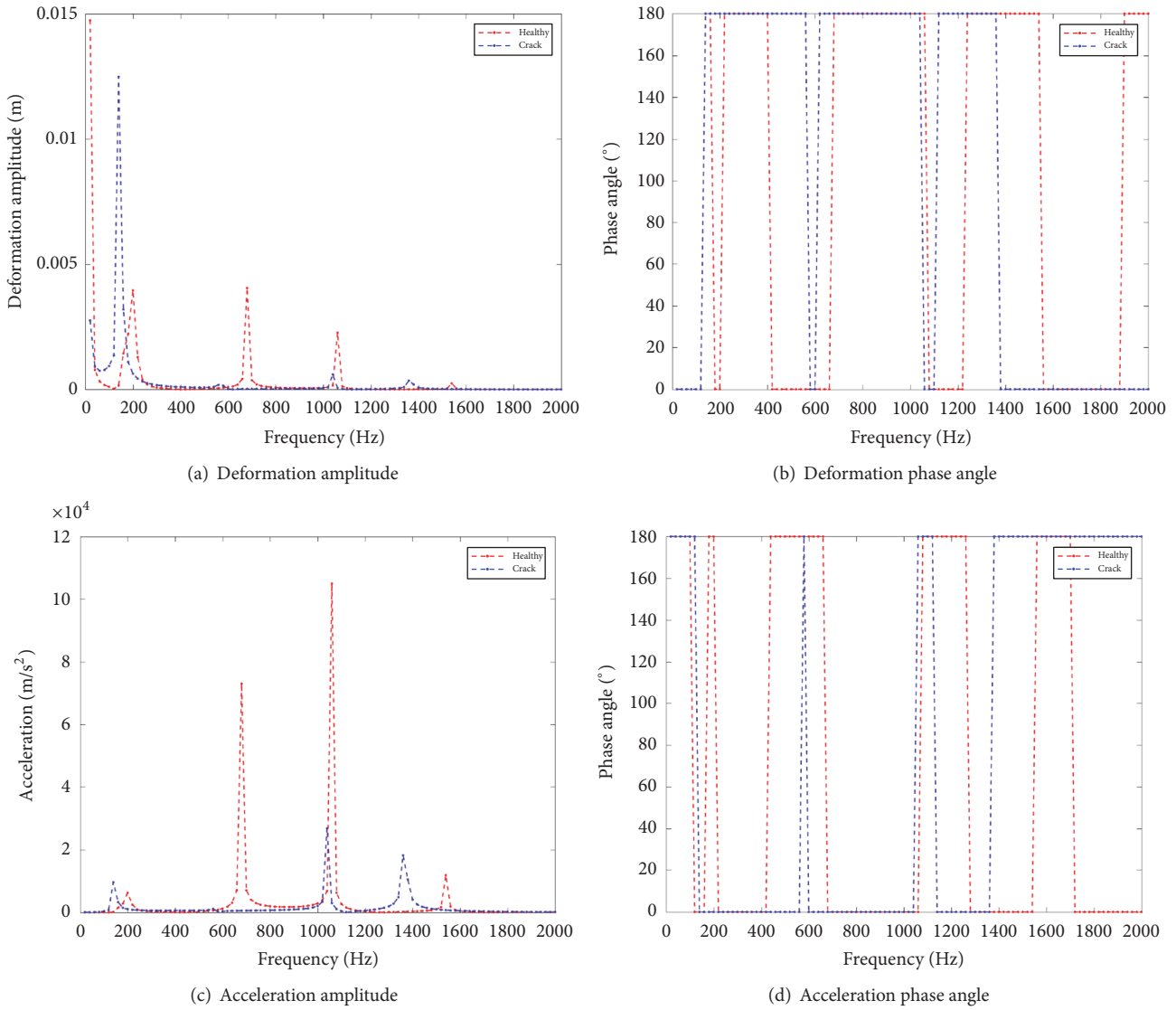

(a) Deformation amplitude

(b) Deformation phase angle

(c) Acceleration amplitude

(d) Acceleration phase angle

Figure 4: Harmonic response spectrum of spiral bevel gear.

In low frequency interval, the tooth fracture model has a significant peak in the deformation amplitude spectrum, while the healthy tooth model has a valley in this interval. However, in the acceleration amplitude spectrum, the peaks of two models are equivalent.

In intermediate frequency interval, the tooth fracture model does not show an obvious peak in deformation and acceleration amplitude spectrum, while the peak value of healthy tooth model is very obvious. And there is no other interference signal in this interval and adjacent interval, so it can be effective in monitoring frequency interval for tooth fracture detection.

In high frequency interval, the acceleration amplitude spectrum is peaked at about 1050 Hz in fracture model, and

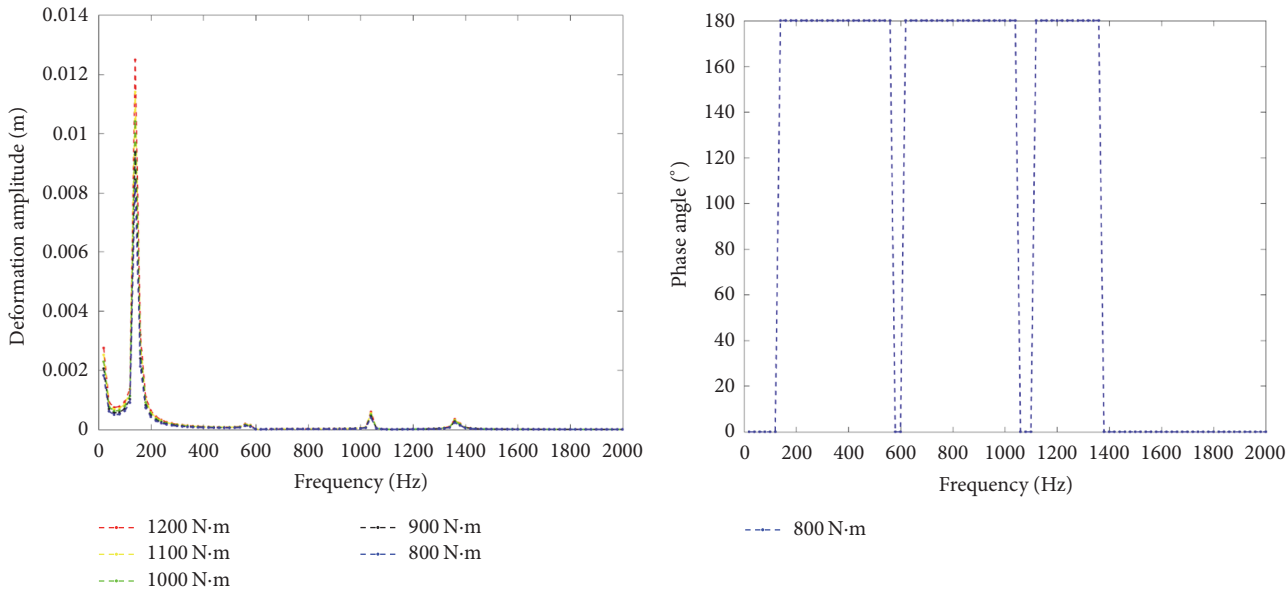

(a) Deformation amplitude

(b) Deformation phase angle

Figure 5: Influence of torque on harmonic response of spiral bevel gear.

the peak of healthy tooth model is four times that of the fracture model.

Compared with Figures 4(a) and 4(c), several peaks of the fracture are in the vicinity of the sidebands of the healthy, and for each corresponding peak, the fracture is less than the healthy; as is shown in Figure 4(a), the peaks also gradually reduce with the increase of the frequency, so high frequency interval cannot easily detect fracture tooth signal. However, acceleration signal is mainly concentrated in intermediate and high frequency intervals.

Compared with Figures 4(b) and 4(d), it can be seen that deformation phase spectrum and acceleration phase spectrum are corresponding to the contrary. And during the sweep process, the phase will be reversed between 0° and 180° in different frequencies. In low frequency interval, the healthy and the fracture coincide and separate from each other quickly, so it is difficult to judge whether the tooth is fractured. The phase mutation inversion is most pronounced at about 600 Hz in the intermediate interval, and it is depicted in both the deformation and acceleration phase spectra. In addition, phase reversal at 1400 Hz in high frequency interval is also relatively obvious.

In brief, low frequency, intermediate frequency, and high frequency interval sections all have tooth fracture characteristic signal; however, the intermediate frequency interval (200 Hz–1000 Hz) is the best interval for detection among others.

3.2. Influence of Torque on Harmonic Response of Spiral Bevel Gear. In order to investigate the effect of torque (dynamic meshing force) and other excitations on the harmonic response of the spiral bevel gear system, tooth fracture model is target object, and the torque of different sizes is loaded without changing the other pretreatment process, so excitation's influence on tooth fracture detection could be obtained. The harmonic response of each load is calculated, respectively, and the result is shown in Figure 5. It can be seen from Figure 5(a) that the torque magnitude has a great influence on the peak value in low frequency interval, and the peak value increases with the torque obviously. However, the torque magnitude has little impact on the intermediate frequency and high frequency intervals. As can be seen from Figure 5(b), the phase spectrum does not change with the increase of torque; that is, torque does not affect the harmonic response phase. This conclusion successfully verifies the experimental test in [12].

3.3. Influence of Measuring Point Position on Harmonic Response of Spiral Bevel Gear. In order to improve the accuracy of the test, the influence of the measuring point position on the harmonic response of the spiral bevel gear system is studied. The responses of the different measuring points are calculated without changing the other pretreatment, so the best monitoring area could be found. The position of the test points is shown in Figure 6, where point A is the measuring point near the working area. The harmonic response spectra of each measurement point are calculated, respectively, and the results are shown in Figure 7. It can be seen from Figure 7(a) that the peak of point C is more obvious in the low frequency interval, and the peak of point A is prominent in the intermediate frequency interval, whereas the vibration of each point is not visible at high frequency interval. According to Figure 7(b), each point has obvious phase mutation inversion at about 600 Hz (intermediate frequency interval) and 1400 Hz (high frequency interval). Based on the above analysis and the conclusion in Section 3.1,

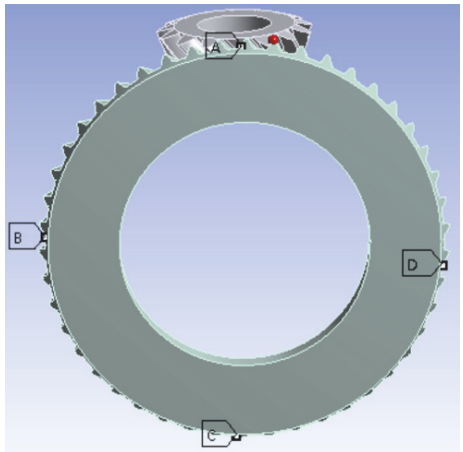

Figure 6: Measuring points position.

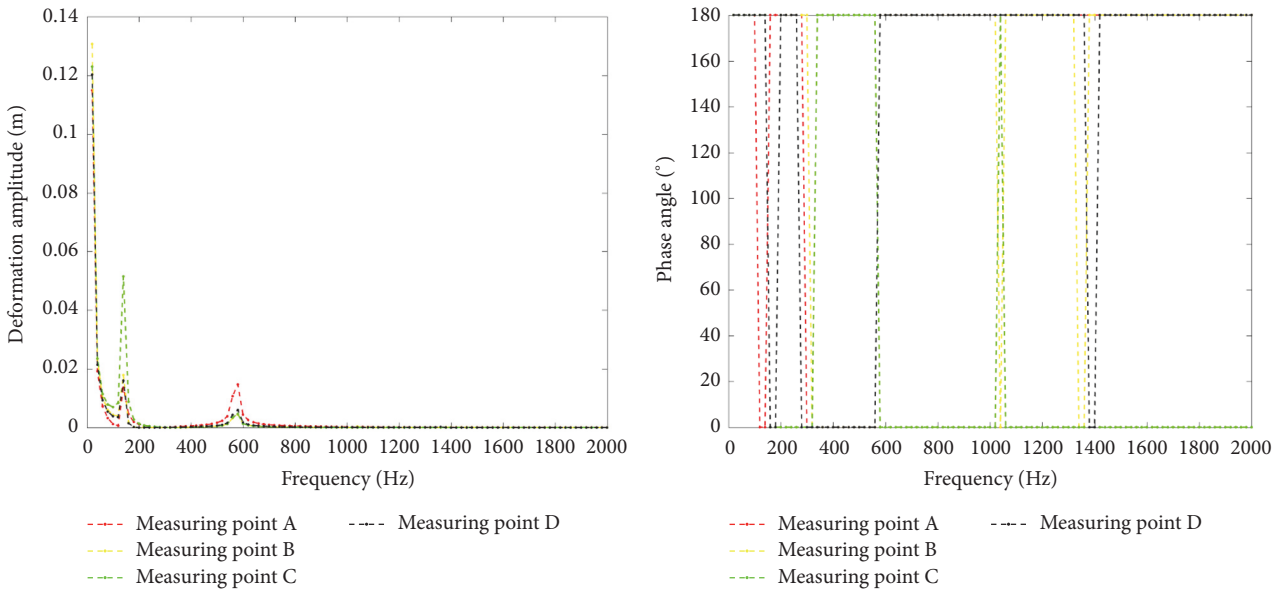

(a) Deformation amplitude

(b) Deformation phase angle

Figure 7: Harmonic responses of spiral bevel gear under different measuring points.

it can be seen that the measuring point near the working area is the best test point when the system is monitored under intermediate frequency interval.

4. Conclusion

Based on the meshing principle and gear cutting process, the tooth involute equation of the bevel gear is obtained, and the parametric spiral bevel gear three-dimensional model and the finite element model are established.

The analysis results draw the following conclusions:

(1) Compared with the healthy tooth model, natural frequency in each order decreases in tooth fracture model, and the natural frequency deviation of the fourth and sixth order is relatively large. Although the low frequency, intermediate frequency, and high frequency interval section have tooth fracture signals, the intermediate frequency interval (200 Hz–1000 Hz) is the best interval to determine whether the tooth is fractured.

(2) The effect of torque on the harmonic response of the spiral bevel gear is quite little, and the change of excitation does not affect the fractured tooth monitoring.

(3) The amplitude of the vibration signal near the working area is relatively strong, and it is the best measuring point area for detecting the fractured tooth signal.

Conflicts of Interest

The authors declare that they have no conflicts of interest.

Acknowledgments

The work described in this paper was fully supported by the National Natural Science Foundation of PRC (Grant nos.

51375226 and 51475226); Postgraduate Research and Practice Innovation Program of Jiangsu Province; China Scholarship Council's support for joint research with Professor Yeping Xiong in University of Southampton.

References

[1] Y. C. Tsai and P. C. Chin, "Surface geometry of straight and spiral bevel gears," *Journal of Mechanisms, Transmissions, and Automation in Design*, vol. 109, no. 4, pp. 443–449, 1987.

[2] F. L. Litvin, A. Fuentes, Q. Fan, and R. F. Handschuh, "Computerized design, simulation of meshing, and contact and stress analysis of face-milled formate generated spiral bevel gears," *Mechanism and Machine Theory*, vol. 37, no. 5, pp. 441–459, 2002.

[3] F. L. Litvin, A. Fuentes, and K. Hayasaka, "Design, manufacture, stress analysis, and experimental tests of low-noise high endurance spiral bevel gears," *Mechanism and Machine Theory*, vol. 41, no. 1, pp. 83–118, 2006.

[4] A. Fuentes, F. L. Litvin, B. R. Mullins, R. Woods, and R. F. Handschuh, "Design and stress analysis of low-noise adjusted bearing contact spiral bevel gears," *Journal of Mechanical Design*, vol. 124, no. 3, pp. 524–532, 2002.

[5] I. Gonzalez-Perez, A. Fuentes, and K. Hayasaka, "Analytical determination of basic machine-tool settings for generation of spiral bevel gears from blank data," *Journal of Mechanical Design*, vol. 132, no. 10, Article ID 101002, 2010.

[6] J. Argyris, A. Fuentes, and F. L. Litvin, "Computerized integrated approach for design and stress analysis of spiral bevel gears," *Computer Methods Applied Mechanics and Engineering*, vol. 191, no. 11-12, pp. 1057–1095, 2002.

[7] G. I. Sheveleva, A. E. Volkov, and V. I. Medvedev, "Algorithms for analysis of meshing and contact of spiral bevel gears," *Mechanism and Machine Theory*, vol. 42, no. 2, pp. 198–215, 2007.

[8] F. L. Litvin, G. I. Sheveleva, D. Vecchiato, I. Gonzalez-Perez, and A. Fuentes, "Modified approach for tooth contact analysis of gear drives and automatic determination of guess values," *Computer Methods Applied Mechanics and Engineering*, vol. 194, no. 27-29, pp. 2927–2946, 2005.

[9] V. Simon, "Computer simulation of tooth contact analysis of mismatched spiral bevel gears," *Mechanism and Machine Theory*, vol. 42, no. 3, pp. 365–381, 2007.

[10] J. Zakrajsek, R. Handschuh, and H. Decker, "Application of fault detection techniques to spiral bevel gear fatigue data," 1994.

[11] P. J. Dempsey, R. F. Handschuh, and A. A. Afjeh, "Spiral bevel gear damage detection using decision fusion analysis," in *Proceedings of the 5th International Conference on Information Fusion*, pp. 94–99, July 2002.

[12] H. Decker and D. Lewicki, "Spiral bevel pinion crack detection in a helicopter gearbox," 2003.

[13] A. Ural, G. Heber, P. A. Wawrzynek, A. R. Ingraffea, D. G. Lewicki, and J. B. C. Neto, "Three-dimensional, parallel, finite element simulation of fatigue crack growth in a spiral bevel pinion gear," *Engineering Fracture Mechanics*, vol. 72, no. 8, pp. 1148–1170, 2005.

[14] M. Li and H. Y. Hu, "Dynamic analysis of a spiral bevel-geared rotor-bearing system," *Journal of Sound and Vibration*, vol. 259, no. 3, pp. 605–624, 2003.

[15] L. Yinong, L. Guiyan, and Z. Ling, "Influence of asymmetric mesh stiffness on dynamics of spiral bevel gear transmission system," *Mathematical Problems in Engineering*, vol. 2010, Article ID 124148, 13 pages, 2010.

[16] Z. Feng and C. Song, "Effects of geometry design parameters on the static strength and dynamics for spiral bevel gear," *International Journal of Rotating Machinery*, vol. 2017, Article ID 6842938, 8 pages, 2017.

[17] Q. Fan, "Computerized modeling and simulation of spiral bevel and hypoid gears manufactured by Gleason face hobbing process," *Journal of Mechanical Design*, vol. 128, no. 6, pp. 1315–1327, 2006.

[18] K. Shi, J. Xia, and C. Wang, "Design of noncircular bevel gear with concave pitch curve," *Proceedings of the Institution of Mechanical Engineers, Part C: Journal of Mechanical Engineering Science*, vol. 227, no. 3, pp. 542–553, 2012.

[19] W. Levine, *The Control Handbook*, CRC Press, Boca Raton, Fla, USA, 1996.